Hydrophilic, Hole-Delocalizing Ligand Shell to Promote Charge Transfer from Colloidal CdSe Quantum Dots in Water

Jonathan R. Lee,[a,b] *Wei Li,*[a,b†] *Alexander J. Cowan,*[b,c] *Frank Jäckel* [a,b]*

[a]Department of Physics, University of Liverpool, Oxford Street, Liverpool, L69 7ZE, UK

[b]Stephenson Institute for Renewable Energy, University of Liverpool, Peach Street, Liverpool, L69 7ZF, UK

[c]Department of Chemistry, University of Liverpool, Crown Street, Liverpool, L69 7ZD, UK

ABSTRACT

Colloidal cadmium chalcogenide nanocrystals are usually stabilized in polar solvents by functionalizing the surface with a layer of hydrophilic ligands. While these ligands protect against aggregation, they also present a steric barrier that hinders surface access. In applications that require charge transfer to and from nanocrystals, colloidal stability and surface access for redox species are therefore difficult to reconcile. This work assesses the possibility of a more dynamic ligand shell that not only provides stability to nanocrystals but also promotes charge transfer without the need for ligand removal. We use transient absorption spectroscopy to study CdSe quantum dots functionalized with hydrophilic, hole-delocalizing dithiocarbamate ligands in water for the first time, and find that a conjugated ligand facilitates charge transfer to redox species in solution.

INTRODUCTION

Energy conversion technologies incorporating semiconductor nanocrystals depend critically on the ability to separate and extract both the electrons and holes that are generated upon photoexcitation. Quantum dot (QD)-sensitized solar cells are limited by the rate at which redox mediators in the electrolyte remove holes from the QDs after electron injection into the oxide scaffold.[1,2] Similarly, in photocatalytic systems, the rate of hole removal from nanocrystals by scavengers dictates the rate of product formation, quantum efficiency.[3–5] An additional concern is that accumulation of holes in nanocrystals eventually results in oxidative degradation, either by ligand removal followed by particle aggregation or by oxidation of the material itself.[3,6]

Increasingly, researchers have begun to focus on the fundamental mechanisms of hole transfer to improve the performance of nanocrystal-based energy systems. Cadmium chalcogenide nanocrystals have been widely investigated and are therefore frequently employed as model light absorbers to which hole acceptors can be covalently bound to control proximity. Tethered ferrocene derivatives attached to CdSe/CdS core/shell nanocrystals by thiol anchoring groups have been used by the Alivisatos group to establish hole transfer rates based on driving force.[7–9] Thiophenols bound to cadmium chalcogenides have been reported to delocalize holes, enhancing QD photostability and extending the lifetime of excited charge carriers.[10–13] The Weiss group has published numerous in-depth studies describing hole delocalization into the ligand shell of QDs, and identified the dithiocarbamate (DTC) functional group as having a particular ability to hybridize extensively with valence band orbitals of cadmium and lead chalcogenides.[14–16] Recently, these authors reported enhanced charge transfer to and from molecular acceptors bound to nanocrystal surfaces via dithiocarbamate linkages.[17,18] Dithiocarbamate functionalization has

also been reported to improve photostability of QDs on TiO_2 and to increase the photoconductivity of QD films.[19,20]

Aqueous photocatalytic systems composed of colloidal nanocrystals present a particular challenge in terms of hole removal. Differences in the passivation of surface traps by various hydrophilic ligands have been shown to significantly influence the quantum efficiency of hydrogen evolution by a CdS/Au photocatalyst.[21] Surface ligands that stabilize individual particles against aggregation and impart solubility also create a barrier that hinders the approach of redox species to the surface. Recent work by our group demonstrated that hydrogen evolution by a CdS/Pt photocatalyst is not observed until the ligand shell is partially compromised through photo-oxidation, and that the duration of hydrogen evolution can subsequently be extended by replacing these ligands in situ with a loosely-bound stabilizer that allows hole scavengers to access the nanocrystal surface.[6] Alternatively, post-synthetic ligand stripping has been shown to enhance activity in nanocrystal-based photocatalysts, but leads to significant particle aggregation in water.[22] A ligand that could promote charge transfer across the nanocrystal/solution interface while bound to the nanocrystal surface, rather than simply providing colloidal stability, would therefore be of interest.

In this work, we present the first transient absorption study of colloidal nanocrystals functionalized with dithiocarbamate ligands in water. We used dithiocarbamates derived from β-alanine (Ala-DTC) and 4-aminobenzoic acid (AmBz-DTC) to investigate the impact of alkyl and aryl DTC ligands on the picosecond charge carrier dynamics of CdSe QDs, and found that band edge electron relaxation occurs up to two orders of magnitude faster than in a typical hydrophilic thiol-coated sample. We further examined these materials in the presence of a commonly used hole scavenger, sodium sulfite, to assess whether DTCs could promote hole scavenging from QDs,

regarded as a rate-limiting step in nanocrystal-based photocatalysis.[3,4] Distinct changes in the bleach recovery kinetics of QDs bearing the aryl-dithiocarbamate ligand Ambz-DTC were observed in the presence of sulfite, consistent with hole scavenging from QDs and a concomitant stabilization of electrons in the conduction band edge state. These results raise the possibility of employing multifunctional ligands in photocatalytic systems that impart colloidal stability and facilitate charge transfer. Where previous reports of related materials have been confined to organic solvents, this work represents a progression towards utilization in aqueous conditions relevant to photocatalysis.

MATERIALS AND EXPERIMENTAL METHODS

Materials.

Cadmium oxide (CdO, PURATRONIC, 99.998%), oleic acid (OA, technical grade, 90%), and trioctylphosphine (TOP, technical grade, 90%) were purchased from Alfa Aesar. 1-octadecene (ODE, technical grade, 90%), selenium powder (~100 mesh, ≥99.5%), β-Alanine (99%), 4-aminobenzoic acid (≥99%), 3-mercaptopropionic acid (MPA, ≥99%), and carbon disulfide (CS_2, ≥99.9%) were purchased from Sigma Aldrich. Sodium sulfite (anhydrous powder), hydrochloric acid, methanol, ethanol, hexane, and chloroform were purchased from Fisher. Tetramethylammonium hydroxide pentahydrate (TMAH, 99%) was purchased from Acros Organics. All reagents were used as received. MilliQ water was produced by an Elga PURELAB Flex purification system.

Synthesis of Quantum Dots.

CdSe QDs were synthesized according to the method of Yu and Peng.[23] 57.6 mg CdO, 0.427 mL OA and 22 mL ODE were combined and vacuum degassed for 30 min at 80 °C, heated

to 300 °C under N_2, then cooled to 250 °C. 64 mg Se powder, 400 µL TOP, and 20 mL ODE were heated under N_2 until all selenium had been dissolved to form a stock solution. 6 mL Se stock solution and 6 mL ODE were vacuum degassed for 30 min at room temperature, then injected into the hot Cd precursor solution. After several minutes, the reaction was removed from heat and allowed to cool to room temperature.

To purify the crude QD product solution, portions were mixed with an equal volume of hexane, then flocculated by addition of ethanol and centrifuged. The colorless supernatant was discarded and the orange CdSe pellet was redispersed in hexane. This cycle was repeated three times before collecting the purified QDs as a concentrated stock solution (10^{-4} M) in chloroform.

Ligand Exchange.

To prepare dithiocarbamate ligand solutions, 360 mg TMAH was dissolved in 1.5 mL MeOH, followed by 1 mmol of either β-alanine or 4-aminobenzoic acid. 80 µL CS_2 was then added dropwise to the amine solution with rapid stirring. Solutions turned yellow, indicating formation of dithiocarbamate. MPA ligand solutions were prepared by adding 1 mmol of the thiol to a solution of 180 mg TMAH in 1.5 mL MeOH. Ligand exchanges were performed by dropwise addition of several hundred microliters of CdSe QD stock in chloroform to the desired ligand solution with rapid stirring at ~0 °C. After equilibration for 3-4 hours, the QD solution was diluted with milliQ water and shaken with several milliliters of chloroform. The aqueous phase was transferred to a Sartorius Vivaspin centrifuge tube and concentrated to several hundred microliters to remove excess ligand and amine precursor impurities from dithiocarbamate formation, then diluted to 2 mL volume with milliQ water. Stock solutions of QDs in water were adjusted to pH 9 using TMAH and HCl, as necessary, measured using a HI 83141 pH probe (Hanna).

As reported elsewhere[14,24], we also observed additional red shifting of the excitonic peak of DTC QDs after ligand exchange. This process was complete after the third day in our experience, so we allowed samples to equilibrate for ~72 hours before performing transient measurements.

Optical Measurements.

Extinction spectra were collected on a Shimadzu UV-2600 spectrophotometer in 10 mm path length quartz cuvettes. Photoluminescence was measured with a Perkin Elmer LS 55 fluorescence spectrometer with 450 nm excitation.

Transient Absorption Spectroscopy.

Femtosecond laser pulses were produced by a PHAROS laser head (Light Conversion, Ltd) using Yb:KGW as the active medium, operated at a repetition rate of 10 kHz. An ORPHEUS optical parametric amplifier (Light Conversion, Ltd) in tandem with a LYRA harmonic generator (Light Conversion, Ltd) produced the desired wavelength for sample excitation. Pump beam intensity was adjusted with a neutral density filter to achieve pulse energies of ~10 nJ/pulse. A portion of the PHAROS output was also used to pump a sapphire crystal to generate a white light continuum for the probe beam, which provided for spectral observation in the region 475-900 nm. The probe beam was focused on the sample to a spot size of ~100 μm diameter and was overlapped completely by the pump beam. Spectra were acquired with a HELIOS transient absorption spectrometer (Ultrafast Systems, LLC) with a response time of ~400 fs (~1.5x the laser pulse length). Datasets were collected by randomly stepping the optical delay line and averaging for 1 s at each delay time. Samples were diluted to an absorbance of 0.6 and measured in a 2 mm path length quartz cuvette fitted with a rubber septum and purged with Ar. Transient spectra were chirp-corrected using the commercial Surface Xplorer (Ultrafast Systems, LLC) software package.

RESULTS AND DISCUSSION

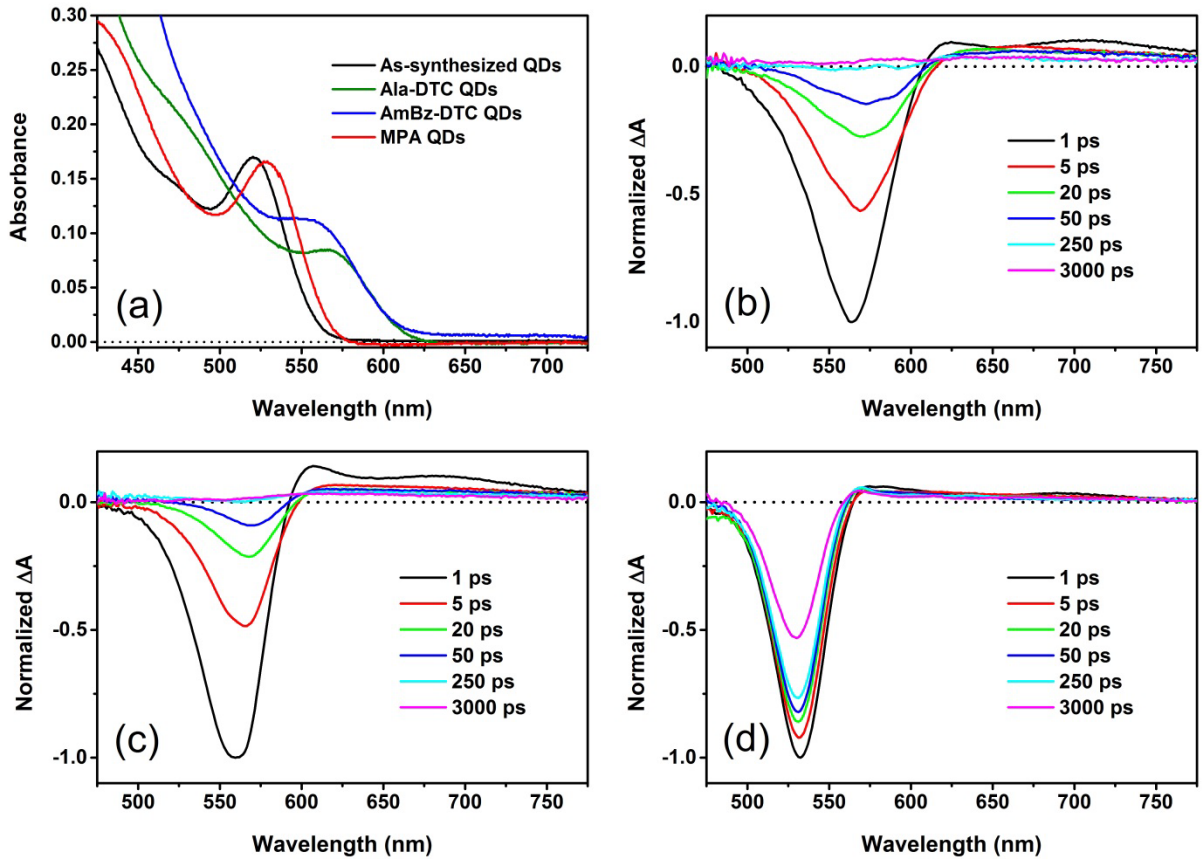

Figure 1. (a) Extinction spectra of as-synthesized QDs in chloroform, and of Ala-DTC, AmBz-DTC, and MPA QDs in water. Transient absorption spectra of (b) Ala-DTC QDs, (c) AmBz-DTC QDs, and (d) MPA QDs at selected time delays, normalized to the maximum intensity of the bleach signal 1 ps after excitation. Horizontal dotted lines represent ΔA equal to zero.

Extinction spectra of the CdSe QDs used in this work are presented in Figure 1a. The excitonic peak at 520 nm for the as-synthesized QDs in chloroform corresponds to an average particle radius of ~1.3 nm.[25] Strong spatial confinement of charge carriers in CdSe QDs is regarded to occur in particles of radii less than ~1.9 nm.[26,27] In this regime, the kinetic energy of the hole

exceeds the Coulomb potential of the electron-hole pair. Using QDs with dimensions well within this range therefore maximizes the degree of hole delocalization upon ligand exchange with DTCs.[15]

The spectra of QDs functionalized with Ala-DTC or AmBz-DTC in Figure 1a exhibit a significant red shift (>150 meV, 35-45 nm) of the excitonic peak; in contrast, MPA induces a more modest shift of ~30 meV (~8 nm). The ligand-induced shift observed in the DTC QDs would correspond to a physical increase in the actual radius of the nanocrystals of ~0.7 nm[25], which is relatively large compared to the shifts reported for PTC adsorption on CdSe QDs in organic solvents. Recent calculations have shown that the magnitude of the red shift of the excitonic peak in cadmium chalcogenide QDs as a result of DTC adsorption increases non-linearly with increasing surface coverage due to electronic coupling between adjacent ligands.[28] The CdSe QDs studied herein were transferred to aqueous solution by a ligand exchange procedure that exposes the particles to a 1000-fold molar excess of dithiocarbamate (or thiol) ligands, so the surface coverage of ligands is expected to be densely functionalized with a high degree of adjacency. The magnitude of the red shift observed here for the DTC QDs is consistent with the predictions of Harris et al. for nearly complete surface coverages[28], although some native ligands likely persist. Ala-DTC QDs exhibit a slightly larger red-shift of the excitonic peak compared to AmBz-DTC QDs, which we attribute to a higher surface density of the less bulky Ala-DTC ligands which permits increased interligand coupling.

We also measured the photoluminescence of the QDs before and after ligand exchange (Figure S1). As-synthesized QDs in chloroform exhibited band edge emission, however this was quenched after ligand exchange in each QD material. In MPA QDs, the band edge emission was reduced to ~4% of its pre-exchange intensity, while emission at longer wavelengths related to

newly-formed trap states appeared to increase slightly, in line with previous observations of MPA-coated CdSe QDs.[29] The photoluminescence of QDs was completely quenched after functionalization with DTC ligands, as reported by other authors.[24,30] Emission quenching is consistent with hole transfer from the nanocrystal core to surface ligands, which has been shown to occur for other hole-accepting ligands adsorbed to CdSe QDs.[31,32] In the case of dithiocarbamates, emission quenching is thought to be related to ligands bound in a monodentate geometry whose lone pairs can efficiently trap holes.[24] The high surface coverage of DTC ligands in the materials studied here likely contributes to the complete quenching of photoluminescence observed.

Transient absorption spectra of CdSe QDs functionalized with Ala-DTC, AmBz-DTC, or MPA are presented in Figures 1b, 1c, and 1d, respectively. Given the spectral shifts that occur upon DTC functionalization, we chose to excite all samples at an energy removed from the region where these changes occur. Samples were therefore pumped with 450 nm laser pulses, exciting the 1P(h)–1P(e) transition.[33,34] Sub-picosecond electron cooling from the hot 1P(e) state to the 1S(e) band edge state subsequently occurs, with parallel processes occurring for holes in the valence band.[24,35] Recent work has shown that adsorbed phenyldithiocarbamate does not affect the electron cooling rate in CdSe QDs, although it does impact hole cooling.[24] The prominent negative signals in the spectra correspond to bleaching of the QD ground state by population of the 1S(e) band edge state, and are conventionally referred to as “B1”, with the decay of this signal tracking the rate at which electrons depopulate the conduction band.[34,36]

The picosecond charge carrier dynamics of MPA-functionalized QDs have been reported previously by numerous authors.[29,35,37] 3-Mercaptopropionic acid (MPA) is perhaps the most widely used hydrophilic thiol for stabilizing colloidal cadmium chalcogenide nanocrystals in

water, as well as for immobilizing QDs on oxide surfaces, so we have included MPA QDs in our study as a benchmark against which DTC-functionalized QDs from the same synthetic batch can be directly compared. In Figure 1d, the ground state bleach signal decays on the nanosecond timescale, indicating a relatively gradual relaxation of electrons from the conduction band. Adsorption of MPA has been shown to create surface traps for both electrons and holes in CdSe QDs[29,37,38], and recombination of 1S(e) electrons with holes trapped at the surface becomes the dominant relaxation pathway in MPA-functionalized QDs leading to the recovery of the ground state bleach.[35] In contrast, functionalization of CdSe QDs with DTC ligands results in the dramatic acceleration of the ground state bleach recovery apparent in Figures 1b and 1c. Such rapid decay of the bleach signal in DTC QDs implies that an efficient relaxation pathway for electrons occupying the 1S(e) state is introduced, such as electron trapping or facilitated electron-hole recombination, associated with the states formed at the QD-ligand interface. Comparing the evolution of the transient spectra in Figure 1, it is clear that dithiocarbamate ligands affect the charge carrier dynamics of CdSe QDs to a much greater extent than MPA.

Positive signals also appear in the transient spectra of all QD samples, consisting of a relatively well-defined peak on the low-energy edge of the bleach and a broader feature that extends into the near-IR; the former is conventionally referred to as “A1” and is associated with biexciton interactions in strongly confined CdSe QDs[34], while the latter photoinduced absorption is labelled “PA” and attributed to lattice- and surface-trapped holes in CdSe QDs.[35,39] We note that these signals overlap in the spectra but can be distinguished according to their shapes. The A1 feature is present in the spectra of MPA QDs, but is not observed in the spectra of DTC QDs after the initial excitation (~1 ps) (Figure S2), which could be due to the reduced wavefunction overlap afforded by hole delocalization into the ligand shell. The broader PA signal relating to trapped

holes appears in the spectra of all QD samples. In the case of DTC QDs, the total recovery of the ground state bleach within several hundred picoseconds means that the PA signal is fully resolved on the nanosecond timescale.

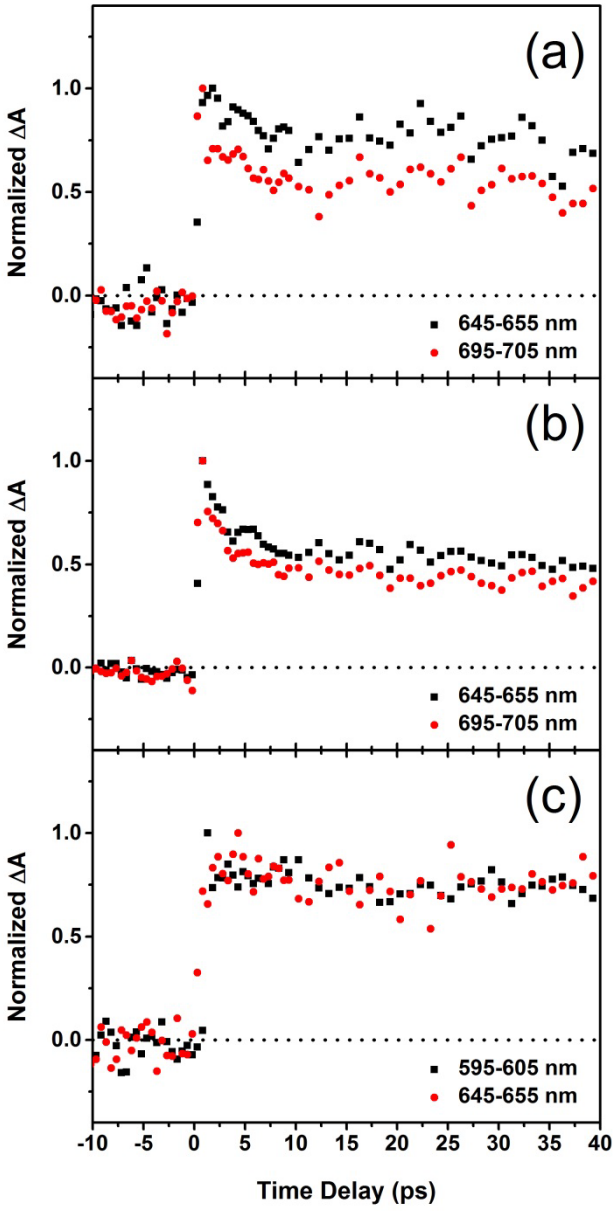

Figure 2. Kinetics of the photoinduced absorption (PA) signal in (a) Ala-DTC, (b) AmBz-DTC, and (c) MPA QDs at early time delays. Values were averaged across the spectral ranges indicated and normalized to the initial signal maximum. Horizontal dotted lines represent ΔA equal to zero.

Hole trapping in CdSe QDs, monitored by the rise time of the PA signal, typically occurs within hundreds of femtoseconds.[24,33,35] Taking the magnitude of this signal at a given time to reflect the population of trapped holes, we compared the kinetics of the PA signal in the different QD materials. Due to the low intensity of the feature, we averaged values across 10 nm regions of the spectrum at each time delay to improve the signal-to-noise ratio of the data. Figure 2 shows the kinetics of the PA signal during the first 50 ps of the transient absorption measurements. In DTC-QDs, the signal related to trapped holes reaches its maximum within <1 ps followed by a rapid decay in the first 10 ps after excitation. Due to the time resolution of our instrument, we cannot investigate sub-picosecond time delays; however, it is likely that the PA signal reaches even higher values in the first several hundred femtoseconds. This picosecond decay process is most pronounced for AmBz-DTC QDs, and is not observed in MPA QDs, which instead have a relatively stable PA signal.

	Ala-DTC		AmBz-DTC		MPA	
λ (nm)	650±5	700±5	650±5	700±5	600±5	650±5
PA_0:$B1_0$	0.082	0.101	0.094	0.096	0.050	0.035

Table 1. Ratios of the magnitudes of the photoinduced absorption (PA) versus the ground state bleach (B1) signals immediately after excitation (PA_0:$B1_0$). PA signal was averaged within the indicated wavelength range.

Given that the intensity of the ground state bleach (B1) is related to the population of 1S(e) electrons and the PA signal corresponds to trapped holes, the ratio of their magnitudes at a given time delay represents a measure of the relative population of these states.[24] In Table 1, we evaluated PA_0 and $B1_0$ as the maximum magnitude of the signals within 5 ps of initial excitation. While the proportion of initially trapped holes appears significantly higher in DTC QDs than in MPA QDs, the fast decay component in the PA signal of DTC QDs implies that holes in a subset of traps in DTC QDs can either readily de-trap or recombine with electrons via a pathway introduced upon DTC functionalization. After several hundred picoseconds, the PA signal is relatively stable in both DTC and MPA QD materials, indicating that some holes remain trapped over longer timescales.[40]

In MPA QDs, the kinetics of the PA signal closely track those of the ground state bleach signal for the duration of the transient measurement (Figure S3), in line with the hypothesis that recombination of 1S(e) electrons with trapped holes is the dominant relaxation process.[35] For DTC QDs, however, this correspondence is observed only in the first 10 picoseconds after excitation, during the period of fast signal decay. Beyond this point, the magnitude of the ground state bleach continues to decrease to zero, unlike the PA signal. As such, the picosecond decay process appears to involve only a fraction of the total population of trapped holes, whereas all 1S(e) electrons are affected by DTC functionalization.

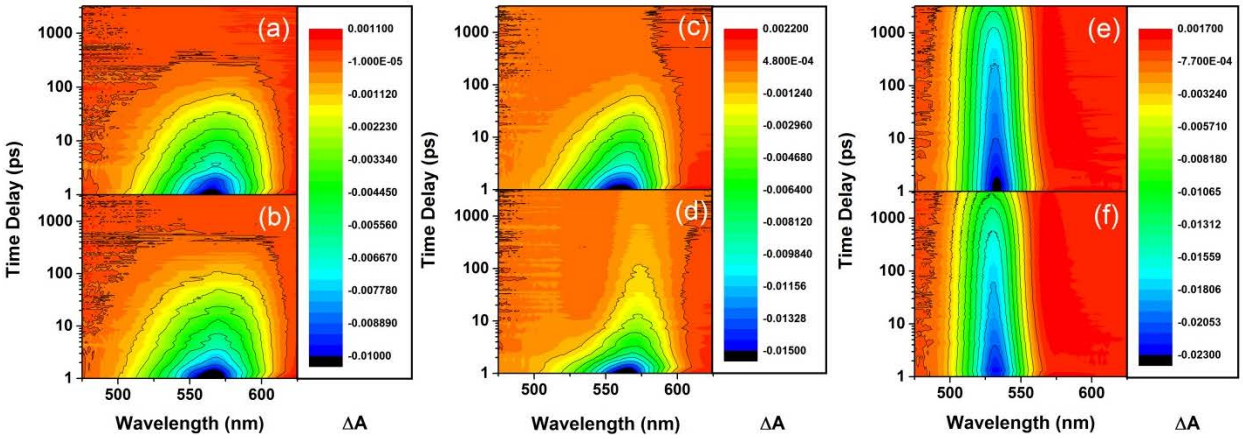

Figure 3. Contour plots detailing the bleach region in the transient absorption spectra of (a) Ala-DTC QDs, (c) AmBz-DTC QDs, (e) MPA QDs. Spectra recorded in the presence of 0.1 M Na_2SO_3 are shown for each material in (b), (d), and (f), respectively.

Considering the valence band of DTC QDs to be extended into the ligand shell[14–16], we hypothesized that this delocalization might facilitate hole scavenging by a redox species in solution and slow depopulation of the 1S(e) state. To test this hypothesis, we collected spectra for all QD samples in the presence of 0.1 M sodium sulfite, a common hole scavenger used in semiconductor nanocrystal-based photocatalysis. Figure 3 presents transient absorption spectra of QD samples in the absence (top row) and presence (bottom row) of sulfite. As is evident from Figures 3c and 3d, sulfite only induced significant changes to the spectrum of AmBz-DTC QDs. Interestingly, rather than affecting the overall spectrum, the addition of sulfite resulted in asymmetric changes to the spectrum at different wavelengths, suggesting that the interaction of sulfite with the QD-ligand complex does not affect the material uniformly but occurs via discrete states.

Due to the quantization of energy levels in QDs, individual spectral features can be assigned to specific transitions between states in the valence and conduction bands.[33,34] In CdSe QDs of the dimensions studied here, the band edge $1S_{3/2}$(h)–1S(e) transition and the higher energy

$2S_{3/2}(h)–1S(e)$ transition are separated by 100-150 meV, and partly overlap to form the characteristic low energy peak in extinction spectra and the B1 bleach feature in transient spectra.[41] We therefore evaluated the kinetics of MPA QDs at 515 nm and 545 nm, and of DTC QDs at 535 nm and 575 nm, consistent with the theoretical energy spacing of the two lowest energy transitions, taking into account the greater separation on the wavelength scale in the red-shifted DTC QD spectra.[35,42]

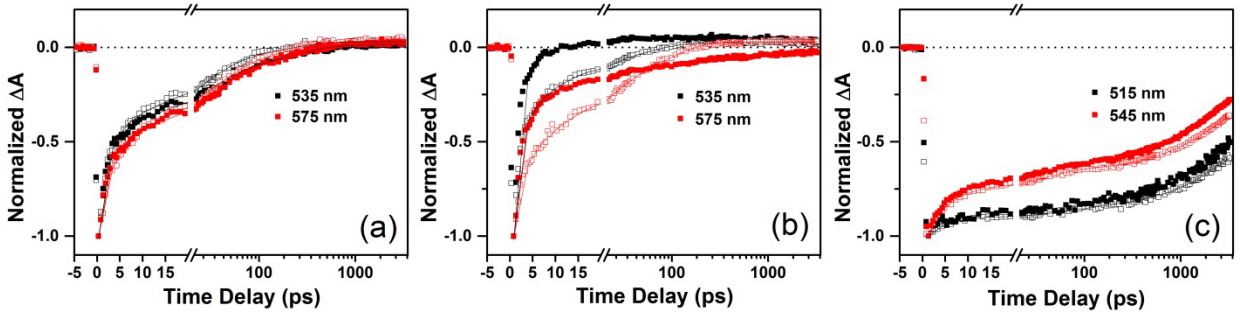

Figure 4. Kinetic plots showing the evolution of the ground state bleach in the absence (open squares) and in the presence (closed squares) of 0.1 M Na_2SO_3, monitored at the wavelengths indicated, for (a) Ala-DTC, (b) AmBz-DTC, and (c) MPA QDs. Note the logarithmic scale after 20 ps time delay. Horizontal dotted lines represent ΔA equal to zero. Solid lines illustrate the triexponential fits used to extract time constants, detailed in Table 2. Additional fitting parameters are detailed in the Supporting Information.

	Ala-DTC QDs				AmBz-DTC QDs				MPA QDs			
	535 nm		575 nm		535 nm		575 nm		515 nm		545 nm	
	Without SO_3^-	*With* SO_3^-	*Without* SO_3^-	*With* SO_3^-	*Without* SO_3^-	*With* SO_3^-	*Without* SO_3^-	*With* SO_3^-	*Without* SO_3^-	*With* SO_3^-	*Without* SO_3^-	*With* SO_3^-
τ_1 (ps)	1.9 ± 0.1	1.5 ± 0.1	2.4 ± 0.1	1.7 ± 0.1	1.0 ± 0.1	0.9 ± 0.1	1.4 ± 0.1	1.5 ± 0.1	3.3 ± 0.5	4.3 ± 1.2	3.5 ± 0.2	3.3 ± 0.2

τ_2 (ps)	22.4 ± 1.3	23.4 ± 1.4	25.7 ± 1.6	25.3 ± 1.2	7.7 ± 0.5	3.3 ± 4.2	12.9 ± 1.0	12.2 ± 0.9	65.5 ± 13.0	75.6 ± 25.1	31.1 ± 2.2	28.7 ± 1.7
τ_3 (ps)	176.0 ± 19.9	211.2 ± 17.7	183.9 ± 18.2	216.0 ± 14.2	45.6 ± 3.2	8.7 ± 4.5	78.3 ± 4.7	310 ± 26	3319 ± 389	3339 ± 606	2634 ± 132	2267 ± 77

Table 2. Time constants derived from triexponential fitting of the ground state bleach recovery kinetics of the QDs, in the absence and presence of 0.1 M Na_2SO_3.

Figure 4 plots the kinetics of the ground state bleach recovery for QDs in the absence and presence of a hole scavenger at wavelengths corresponding to the $1S_{3/2}(h)$–1S(e) and $2S_{3/2}(h)$–1S(e) transitions. These kinetics were fit to triexponentials to extract time constants to describe the decay processes, which are detailed in Table 2. Differences exist in the relative rates of $1S_{3/2}(h)$–1S(e) and $2S_{3/2}(h)$–1S(e) bleach recovery among the samples even in the absence of sulfite. In AlaDTC QDs, these two transitions recover at nearly identical rates, while in AmBzDTC QDs the $2S_{3/2}(h)$–1S(e) transition recovers roughly twice as fast as the lower energy transition. The availability of vibrational modes in AmBzDTC associated with the aromatic ring, which are not available in AlaDTC, might contribute to faster relaxation of the $2S_{3/2}(h)$–1S(e) transition.[43] It is also possible that some variation exists in the binding geometries adopted by the smaller AlaDTC and the larger, more rigid AmBzDTC in the crowded ligand shells, which has been shown to affect relaxation rates.[24,44,45] By comparison, MPA QD bleach recovery is at least ten times slower than in the DTC-functionalized materials, with the $1S_{3/2}(h)$–1S(e) transition recovering marginally faster than $2S_{3/2}(h)$–1S(e), reflecting different underlying QD-ligand interactions.

Figure 4b shows that sulfite accelerates the recovery of the bleached $2S_{3/2}(h)$–1S(e) transition at 535 nm in AmBz-DTC QDs, by an order of magnitude overall as quantified by the τ_2

and τ_3 time constants. Indeed, it can be seen in the plot that the signal drops to zero after just ~10 ps in the presence of sulfite, compared to ~100 ps in the absence of the hole scavenger. Concurrently, after a similarly fast decay at early delay times, the recovery of the bleached band edge transition at 575 nm slows markedly, manifesting as a four-fold increase in τ_3 time constant. This asymmetric effect of sulfite on the transient spectrum of AmBz-DTC QDs is notably absent for Ala-DTC and MPA QDs, where only modest changes in time constants are observed, on the order of the standard errors of the fits. Most significantly, the bleaching of the band edge transition at 575 nm now persists into the nanosecond timescale in the presence of sulfite, indicating a substantial increase in the lifetime of 1S(e) conduction band electrons in AmBz-DTC QDs. These kinetics are presented on a linear scale in Figure S5 to emphasize the extended 1S(e) lifetime.

Given that excitation of the $1S_{3/2}$(h)–1S(e) and $2S_{3/2}$(h)–1S(e) transitions populates the same conduction band state, any discrepancy in the recovery kinetics of the bleach signal at the wavelengths associated with these transitions implies a difference in the dynamics of their respective hole states. Such state-specificity involving the $2S_{3/2}$(h) state in CdSe QDs has been observed following adsorption of phenyldithiocarbate[46] as well as hole-accepting catechols[31] and thiols[32], and ascribed to hot hole transfer. Unfortunately, the lack of a clear spectroscopic signature for valence band holes in CdSe QDs means that we cannot directly probe these states; however, the fact that different recovery kinetics arise in AmBz-DTC QDs only in the presence of a hole scavenger, and that in this case it is the lifetime of the transient signal associated with conduction band electrons that is extended, offers strong indirect evidence that the conjugated, hole-delocalizing ligands can promote charge transfer between the nanocrystals and redox species in solution.

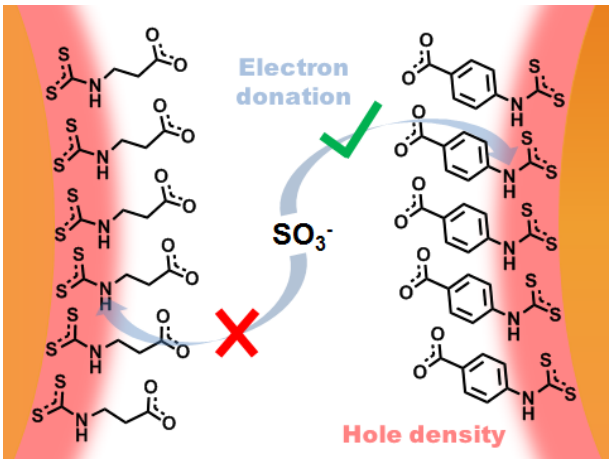

Figure 5. Schematic representation of QD-ligand-solution interfaces in Ala-DTC and AmBz-DTC QDs. Holes delocalized onto dithiocarbamate anchoring groups are isolated at the interface by the alkyl backbone of Ala-DTC, but are accessible to sulfite due to the aromatic bridge of AmBz-DTC.

Ala-DTC QDs provide a useful point of comparison from which to explore possible mechanisms to explain the response of AmBz-DTC QDs to sulfite. Ala-DTC and AmBz-DTC both adsorb to CdSe QDs via the same functional group, resulting in similar red shifts of their excitonic peaks in extinction spectra and faster bleach recovery kinetics in general. Calculations by Azpiroz and De Angelis have shown that the orbitals into which hole density primarily delocalizes are on the dithiocarbamate group in such systems, not the aryl group, so it follows that qualitatively similar behavior should be observed for both ligands.[45] The aromatic ring in AmBz-DTC can however conjugate to the dithiocarbamate group; in contrast, an alkyl chain isolates the dithiocarbamate group in Ala-DTC at the QD interface, with MPA having an analogous structure. Jin and co-workers previously reported that a bifunctional conjugated dithiocarbamate linker facilitated electron transfer from a photoexcited porphyrin to CdSe QDs.[17] Work from the same

group has also demonstrated hole transfer from a CdS QD to a molecular acceptor via a conjugated dithiocarbamate binding group.[18] Similarly, it is thought the conjugation of the AmBzDTC ligand facilitates electron transfer from sulfite to the dithiocarbamate group where holes are delocalized.

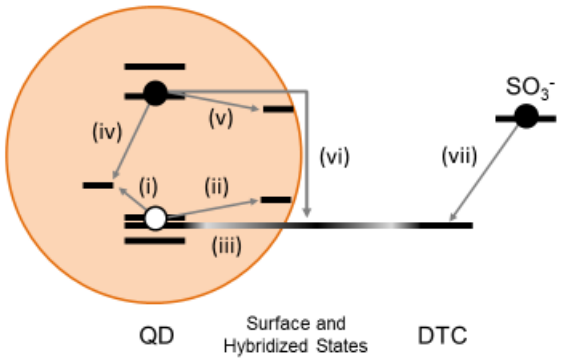

Figure 6. Summary of the proposed processes responsible for the observed charge carrier dynamics in DTC QDs. (i) Hole trapping to core states; (ii) hole trapping to surface states; (iii) hole delocalization into hybridized QD-DTC states; (iv) hole trap-mediated recombination, governs relaxation in MPA QDs; (v) electron trapping; (vi) electron-hole recombination via hybridized QD-DTC states; (vii) electron transfer (hole scavenging) by sulfite in solution.

Based on the spectroscopic features discussed above, several processes appear to govern the charge carrier dynamics in DTC QDs in aqueous conditions, summarized in Figure 6. Upon excitation, an electron-hole pair is created in the CdSe QD core, with electrons populating 1S(e) conduction band states of predominantly QD character in the core.[45] This process results in the appearance of the ground state bleach signal, which recovers on the order of tens of picoseconds as electrons begin to depopulate the conduction band. Within 1 ps of excitation, some valence band holes are trapped at lattice or surface sites, giving rise to the PA signal, while others delocalize in

hybridized QD-ligand states. Delocalization of holes beyond the volume of the QD core would induce electron migration to the surface of the QD as a result of Coulomb drag[47], bringing electrons into closer proximity with surface trapped holes. Electrons could recombine with these trapped holes, leading to the observed picosecond decay in the PA signal of DTC QDs, or be trapped themselves in surface states arising from QD-DTC interactions.[24] Both of these processes would depopulate the 1S(e) state and contribute to recovery of the ground state bleach. Finally, in the presence of sulfite, the rate of depopulation of the conduction band can be slowed by a factor of four, effectively increasing the lifetime of excited electrons in QDs functionalized with the conjugated dithiocarbamate ligand, AmBz-DTC.[48]

CONCLUSIONS

We have described for the first time the picosecond charge carrier dynamics of colloidal CdSe QDs stabilized in water by hydrophilic dithiocarbamate ligands. Using transient absorption spectroscopy, we observed the recovery kinetics of the QD ground state bleach to be vastly accelerated compared to those of thiol-functionalized QDs. Further, we demonstrate that in the presence of a hole scavenger in solution, the lifetime of electrons in the band edge excited state is extended, suggesting that holes have been transferred without hindrance by the layer of stabilizing ligands. These findings have relevance in several fields that rely on charge transfer to and from semiconductor nanocrystals, such as quantum dot-sensitized solar cells and nanocrystal-based photocatalytic systems.

ASSOCIATED CONTENT

Supporting Information. Photoluminescence of QDs before and after ligand exchange, detail of photoinduced absorption spectral regions, comparison of B1 and PA kinetics, PA kinetics in the presence of sulfite, and bleach kinetics of AmBz-DTC QDs plotted on a linear scale.

The following files are available free of charge:

Supporting Information (PDF)

AUTHOR INFORMATION

Corresponding Author

*E-mail: fjaeckel@liverpool.ac.uk

Present Address

[†]Chemical Engineering & Applied Chemistry, European Bioenergy Research Institute and Aston Materials Centre, Aston University, Aston Triangle, Birmingham B4 7ET, UK

Author Contributions

The manuscript was written through contributions of all authors. All authors have given approval to the final version of the manuscript.

Notes

The authors declare no competing financial interests.

ACKNOWLEDGMENTS

Financial support by The University of Liverpool (F.J.) is gratefully acknowledged. J.L. thanks the School of Physical Sciences for support through a GTA studentship. The authors further acknowledge support from the EPSRC Laser Loan Pool (EP/G03088X/1). The underlying EPSRC-funded data in this paper is available from (insert hyperlink pending DOI).

REFERENCES

(1) Kamat, P. V; Christians, J. A.; Radich, J. G. Quantum Dot Solar Cells: Hole Transfer as a Limiting Factor in Boosting the Photoconversion Efficiency. *Langmuir* **2014**, *30*, 5716–5725.

(2) Abdellah, M.; Marschan, R.; Zidek, K.; Messing, M. E.; Abdelwahab, A.; Chabera, P.; Zheng, K.; Pullerits, T. Hole Trapping: The Critical Factor for Quantum Dot Sensitized Solar Cell Performance. *J. Phys. Chem. C* **2014**, *118*, 25802–25808.

(3) Berr, M. J.; Wagner, P.; Fischbach, S.; Vaneski, A.; Schneider, J.; Susha, A. S.; Rogach, A. L.; Jäckel, F.; Feldmann, J. Hole Scavenger Redox Potentials Determine Quantum Efficiency and Stability of Pt-Decorated CdS Nanorods for Photocatalytic Hydrogen Generation. *Appl. Phys. Lett.* **2012**, *100*, 223903.

(4) Wu, K.; Chen, Z.; Lv, H.; Zhu, H.; Hill, C. L.; Lian, T. Hole Removal Rate Limits Photodriven H_2 Generation Efficiency in CdS-Pt and CdSe/CdS-Pt Semiconductor Nanorod-Metal Tip Heterostructures. *J. Am. Chem. Soc.* **2014**, *136*, 7708–7716.

(5) Simon, T.; Bouchonville, N.; Berr, M. J.; Vaneski, A.; Adrović, A.; Volbers, D.; Wyrwich, R.; Döblinger, M.; Susha, A. S.; Rogach, A. L.; Jäckel, F.; Stolarczyk, J. K.; Feldmann, J. Redox Shuttle Mechanism Enhances Photocatalytic H_2 Generation on Ni-Decorated CdS Nanorods. *Nat. Mater.* **2014**, *13*, 1013–1018.

(6) Li, W.; Lee, J. R.; Jäckel, F. Simultaneous Optimization of Colloidal Stability and Interfacial Charge Transfer Efficiency in Photocatalytic Pt/CdS Nanocrystals. *ACS Appl. Mater. Interfaces* **2016**, *8*, 29434–29441.

(7) Tarafder, K.; Surendranath, Y.; Olshansky, J. H.; Alivisatos, A. P.; Wang, L. W. Hole Transfer Dynamics from a CdSe/CdS Quantum Rod to a Tethered Ferrocene Derivative. *J. Am. Chem. Soc.* **2014**, *136*, 5121–5131.

(8) Olshansky, J. H.; Ding, T. X.; Lee, Y. V.; Leone, S. R.; Alivisatos, A. P. Hole Transfer from Photoexcited Quantum Dots: The Relationship between Driving Force and Rate. *J. Am. Chem. Soc.* **2015**, *137*, 15567–15575.

(9) Ding, T. X.; Olshansky, J. H.; Leone, S. R.; Alivisatos, A. P. On the Efficiency of Hole Transfer from Photoexcited Quantum Dots to Covalently Linked Molecular Species On the Efficiency of Hole Transfer from Photoexcited Quantum Dots to Covalently Linked Molecular Species. *J. Am. Chem. Soc.* **2015**, *137*, 2021–2029.

(10) Liu, I. S.; Lo, H.-H.; Chien, C.-T.; Lin, Y.-Y.; Chen, C.-W.; Chen, Y.-F.; Su, W.-F.; Liou, S.-C. Enhancing Photoluminescence Quenching and Photoelectric Properties of CdSe Quantum Dots with Hole Accepting Ligands. *J. Mater. Chem.* **2008**, *18*, 675–682.

(11) Liang, Y.; Thorne, J. E.; Parkinson, B. A. Controlling the Electronic Coupling between

CdSe Quantum Dots and Thiol Capping Ligands via pH and Ligand Selection. *Langmuir* **2012**, *28*, 11072–11077.

(12) Aruda, K. O.; Amin, V. A.; Thompson, C. M.; Lau, B.; Nepomnyashchii, A. B.; Weiss, E. A. Description of the Adsorption and Exciton Delocalizing Properties of p-Substituted Thiophenols on CdSe Quantum Dots. *Langmuir* **2016**, *32*, 3354–3364.

(13) Tan, Y.; Jin, S.; Hamers, R. J. Influence of Hole-Sequestering Ligands on the Photostability of CdSe Quantum Dots. *J. Phys. Chem. C* **2013**, *117*, 313–320.

(14) Frederick, M. T.; Weiss, E. A. Relaxation of Exciton Confinement in CdSe Quantum Dots by Modification with a Conjugated Dithiocarbamate Ligand. *ACS Nano* **2010**, *4*, 3195–3200.

(15) Frederick, M. T.; Amin, V. A.; Cass, L. C.; Weiss, E. A. A Molecule to Detect and Perturb the Confinement of Charge Carriers in Quantum Dots. *Nano Lett.* **2011**, *11*, 5455–5460.

(16) Frederick, M. T.; Amin, V. A.; Swenson, N. K.; Ho, A. Y.; Weiss, E. A. Control of Exciton Confinement in Quantum Dot−Organic Complexes through Energetic Alignment of Interfacial Orbitals. *Nano Lett.* **2013**, *13*, 287–292.

(17) Jin, S.; Tagliazucchi, M.; Son, H.-J.; Harris, R. D.; Aruda, K. O.; Weinberg, D. J.; Nepomnyashchii, A. B.; Farha, O. K.; Hupp, J. T.; Weiss, E. A. Enhancement of the Yield of Photoinduced Charge Separation in Zinc Porphyrin–Quantum Dot Complexes by a Bis(dithiocarbamate) Linkage. *J. Phys. Chem. C* **2015**, *119*, 5195–5202.

(18) Lian, S.; Weinberg, D. J.; Harris, R. D.; Kodaimati, M. S.; Weiss, E. A. Subpicosecond Photoinduced Hole Transfer from a CdS Quantum Dot to a Molecular Acceptor Bound

Through an Exciton-Delocalizing Ligand. *ACS Nano* **2016**, *10*, 6372–6382.

(19) Tan, Y.; Jin, S.; Hamers, R. J. Photostability of CdSe Quantum Dots Functionalized with Aromatic Dithiocarbamate Ligands. *ACS Appl. Mater. Interfaces* **2013**, *5*, 12975–12983.

(20) Zotti, G.; Vercelli, B.; Berlin, A.; Virgili, T. Multilayers of CdSe Nanocrystals and Bis(dithiocarbamate) Linkers Displaying Record Photoconduction. *J. Phys. Chem. C* **2012**, *116*, 25689–25693.

(21) Ben-Shahar, Y.; Scotognella, F.; Waiskopf, N.; Kriegel, I.; Dal Conte, S.; Cerullo, G.; Banin, U. Effect of Surface Coating on the Photocatalytic Function of Hybrid CdS-Au Nanorods. *Small* **2015**, *11*, 462–471.

(22) Chang, C. M.; Orchard, K. L.; Martindale, B. C. M.; Reisner, E. Ligand Removal from CdS Quantum Dots for Enhanced Photocatalytic H_2 Generation in pH Neutral Water. *J. Mater. Chem. A* **2016**, *4*, 2856–2862.

(23) Yu, W. W.; Peng, X. Formation of High-Quality CdS and Other II-VI Semiconductor Nanocrystals in Noncoordinating Solvents: Tunable Reactivity of Monomers. *Angew. Chem. Int. Ed. Engl.* **2002**, *41*, 2368–2371.

(24) Azzaro, M. S.; Babin, M. C.; Stauffer, S. K.; Henkelman, G.; Roberts, S. T. Can Exciton-Delocalizing Ligands Facilitate Hot Hole Transfer from Semiconductor Nanocrystals? *J. Phys. Chem. C* **2016**, *120*, 28224–28234.

(25) Yu, W. W.; Qu, L.; Guo, W.; Peng, X. Experimental Determination of the Extinction Coefficient of CdTe , CdSe , and CdS Nanocrystals. *Chem. Mater.* **2003**, *15*, 2854–2860.

(26) Takagahara, T. Biexciton States in Semiconductor Quantum Dots and Their Nonlinear

Optical Properties. *Phys. Rev. B* **1989**, *39*, 10206–10231.

(27) Achermann, M.; Hollingsworth, J. A.; Klimov, V. I. Multiexcitons Confined within a Sub-Excitonic Volume: Spectroscopic and Dynamical Signatures of Neutral and Charged Biexcitons in Ultrasmall Semiconductor Nanocrystals. *Phys. Rev. B* **2003**, *68*, 245302.

(28) Harris, R. D.; Amin, V. A.; Lau, B.; Weiss, E. A. Role of Interligand Coupling in Determining the Interfacial Electronic Structure of Colloidal CdS Quantum Dots. *ACS Nano* **2016**, *10*, 1395–1403.

(29) Baker, D. R.; Kamat, P. V. Tuning the Emission of CdSe Quantum Dots by Controlled Trap Enhancement. *Langmuir* **2010**, *26*, 11272–11276.

(30) Jin, S.; Harris, R. D.; Lau, B.; Aruda, K. O.; Amin, V. A.; Weiss, E. A. Enhanced Rate of Radiative Decay in CdSe Quantum Dots upon Adsorption of an Exciton-Delocalizing Ligand. *Nano Lett.* **2014**, *14*, 5323–5328.

(31) Singhal, P.; Ghosh, H. N. Hot-Hole Extraction from Quantum Dot to Molecular Adsorbate. *Chem. - A Eur. J.* **2015**, *21*, 4405–4412.

(32) Singhal, P.; Ghorpade, P. V.; Shankarling, G. S.; Singal, N.; Jha, S. K.; Tripathi, R. M.; Ghosh, H. N. Exciton Delocalization and Hot Hole Extraction in CdSe QDs and CdSe/ZnS Type 1 Core Shell QDs Sensitized with Newly Synthesized Thiols. *Nanoscale* **2016**, *8*, 1823–1833.

(33) Kambhampati, P. Unraveling the Structure and Dynamics of Excitons in Semiconductor Quantum Dots. *Acc. Chem. Res.* **2011**, *44*, 1–13.

(34) Klimov, V. I. Spectral and Dynamical Properties of Multiexcitons in Semiconductor

Nanocrystals. *Annu. Rev. Phys. Chem.* **2007**, *58*, 635–673.

(35) Schnitzenbaumer, K. J.; Labrador, T.; Dukovic, G. Impact of Chalcogenide Ligands on Excited State Dynamics in CdSe Quantum Dots. *J. Phys. Chem. C* **2015**, *119*, 13314–13324.

(36) Huang, J.; Huang, Z.; Yang, Y.; Zhu, H.; Lian, T. Multiple Exciton Dissociation in CdSe Quantum Dots by Ultrafast Electron Transfer to Adsorbed Methylene Blue. *J. Am. Chem. Soc.* **2010**, *132*, 4858–4864.

(37) Zheng, K.; Žídek, K.; Abdellah, M.; Zhang, W.; Chábera, P.; Lenngren, N.; Yartsev, A.; Pullerits, T. Ultrafast Charge Transfer from CdSe Quantum Dots to P-Type NiO: Hole Injection vs Hole Trapping. *J. Phys. Chem.* **2014**, *118*, 18462–18471.

(38) Lenngren, N.; Abdellah, M.; Zheng, K.; Al-Marri, M. J.; Zigmantas, D.; Žídek, K.; Pullerits, T. Hot Electron and Hole Dynamics in Thiol-Capped CdSe Quantum Dots Revealed by 2D Electronic Spectroscopy. *Phys. Chem. Chem. Phys.* **2016**, *18*, 26199–26204.

(39) Huang, J.; Huang, Z.; Jin, S.; Lian, T. Exciton Dissociation in CdSe Quantum Dots by Hole Transfer to Phenothiazine. *J. Phys. Chem. C* **2008**, *112*, 19734–19738.

(40) Abdellah, M.; Karki, K. J.; Lenngren, N.; Zheng, K.; Pascher, T.; Yartsev, A.; Pullerits, T. Ultra Long-Lived Radiative Trap States in CdSe Quantum Dots. *J. Phys. Chem. C* **2014**, *118*, 21682–21686.

(41) Klimov, V. I.; McBranch, D. W.; Leatherdale, C. A.; Bawendi, M. G. Electron and Hole Relaxation Pathways in Semiconductor Quantum Dots. *Phys. Rev. B* **1999**, *60*, 13740–13749.

(42) Norris, D. J.; Bawendi, M. G. Measurement and Assignment of the Size-Dependent Optical

Spectrum in CdSe Quantum Dots. *Phys. Rev. B* **1996**, *53*, 16338–16346.

(43) Swenson, N. K.; Ratner, M. A.; Weiss, E. A. Computational Study of the Enhancement of Raman Signals of Ligands Adsorbed to CdSe Clusters through Photoexcitation of the Cluster. *J. Phys. Chem. C* **2016**, *120*, 20954–20960.

(44) Swenson, N. K.; Ratner, M. A.; Weiss, E. A. Computational Study of the Influence of the Binding Geometries of Organic Ligands on the Photoluminescence Quantum Yield of CdSe Clusters. *J. Phys. Chem. C* **2016**, *120*, 6859–6868.

(45) Azpiroz, J. M.; De Angelis, F. Ligand Induced Spectral Changes in CdSe Quantum Dots. *ACS Appl. Mater. Interfaces* **2015**, *7*, 19736–19745.

(46) Xie, Y.; Teunis, M. B.; Pandit, B.; Sardar, R.; Liu, J. Molecule-like CdSe Nanoclusters Passivated with Strongly Interacting Ligands: Energy Level Alignment and Photoinduced Ultrafast Charge Transfer Processes. *J. Phys. Chem. C* **2015**, *119*, 2813–2821.

(47) Mauser, C.; Da Como, E.; Baldauf, J.; Rogach, A. L.; Huang, J.; Talapin, D. V.; Feldmann, J. Spatio-Temporal Dynamics of Coupled Electrons and Holes in Nanosize CdSe-CdS Semiconductor Tetrapods. *Phys. Rev. B* **2010**, *82*, 81306.

(48) Berr, M. J.; Vaneski, A.; Mauser, C.; Fischbach, S.; Susha, A. S.; Rogach, A. L.; Jäckel, F.; Feldmann, J. Delayed Photoelectron Transfer in Pt-Decorated CdS Nanorods under Hydrogen Generation Conditions. *Small* **2012**, *8*, 291–297.

Table of Contents Graphic

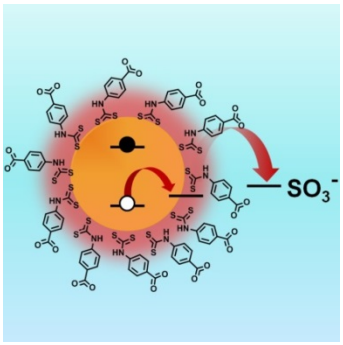
SO3-